Final Technical Report

Project Title: Green, stable and earth abundant ionic PV absorbers based on chalcogenide perovskite

Project Period: (5/1/2016-10/31/2017)

Reporting Period: final

Reporting Frequency: Final

Submission Date: (01/10/18)

Recipient: The Research Foundation for SUNY on behalf of U. at Buffalo

Recipient DUNS #: 038633251

Address: P.O. BOX 9
ALBANY NY 122010009

Website (if available) www.buffalo.edu

Award Number: DE-EE0007364

Awarding Agency: DOE EERE SIPS PV subprogram

Working Partners: Rensselaer Polytechnic Institute

Cost-Sharing Partners: Rensselaer Polytechnic Institute

Principal Investigator: Hao Zeng
Professor
Phone: 716-645-2946
Fax: 716-645-2017
Email: haozeng@buffalo.edu

Submitted by: (if other than PI) Hao Zeng

DOE Contracting Officer: Diana Bobo

DOE Project Manager: Christopher Anderson

_____ _____**01/15/2018**_____

Signature **Date**

Award Number: [*DE-EE0007364*]

Executive summary

Searching for inexpensive, environment-friendly, and air-stable absorber materials for thin film solar cells has become a key thrust of PV research. Supported by this one-year award, the UB-RPI team aims to develop a novel class of semiconductors — chalcogenide perovskites. Sharing some similarities to the widely researched halide perovskites, and unlike most conventional semiconductors, the chalcogenide perovskites are strongly ionic. Such characteristics is expected to provide intrinsic defect properties favorable for charge transport in PV absorbers. In this one-year project, we confirmed structural stability of the $BaZrS_3$ material through high pressure Raman studies. We find no evidence that the perovskite structure of $BaZrS_3$ undergoes any phase changes under hydrostatic pressure to at least 8.9 GPa. Our results indicate the robust structural stability of $BaZrS_3$, and suggest cation alloying as a viable approach for band-gap engineering for photovoltaic and other applications. We also achieved reduced band gap to 1.45 eV by Ti-alloying of $BaZrS_3$, which is close to the optimal value for a single junction solar cell. We further synthesized $BaZrS_3$ thin films with desired crystal structure and band gap. The optical absorption is high as expected. The carrier mobility is moderate. The high processing temperature limits its ability for device integration. We are working on deposition of chalcogenide perovskite thin films using molecular beam epitaxy.

Table of Contents

Background: The recent development of organic halide perovskites such as $CH_3NH_3PbI_3$ has led to a revolution in PV research. The power conversion efficiency (PCE) of solar cells made of this type of materials has witnessed an unprecedented rate of increase, from an initial PCE of 3.8% in 2009[1] to 22.7% in 2017,[2] on par with that achieved in single crystal Si solar cells.

Despite the surge in interest in organic halide perovskite materials, there is still a long way to go for their large-scale commercial applications. The major challenges are 1) the material contains toxic element Pb; 2) the material dissociates rapidly in the presence of moisture;[3] 3) ion migration leading to long-term stability concern;[4] 4) ultralow thermal conductivity potentially leading to heating and mechanical stress.[5] While some of these issues are being addressed by the research community, some appear to be intrinsic to the organic lead halide that cannot be easily solved.

The progress on halide perovskites has inspired us to search for novel semiconductor materials that can inherit the excellent optoelectronic properties of halides, while avoiding their severe limitations. We notice that different from conventional covalent semiconductors, halide perovskite represents the first non-four-coordinate structure with excellent carrier transport and optoelectronic properties. As opposed to their oxide and halide siblings, chalcogenide perovskites received little attention.[6-9] Recently, our theoretical investigation and later experimental works on this type of perovskites have led to some exciting discoveries:[10-13] 1) Among the three different phases of this class of materials, many are semiconductors with band gaps ranging from 0.5 eV to 2.3 eV depending on composition; 2) In the distorted perovskite phase, the material is direct band gap with high optical absorption coefficients; 3) The band dispersion near band edge is large suggesting good carrier mobility; 4) Due to strong iconicity, the materials are expected to be free of deep-level defects, which is the main contributor to carrier recombination. If these results experimentally verified, chalcogenide perovskites may be the ultimate PV absorber material people are searching for.

Introduction: Based on our previous work, we propose a joint experimental and theoretical program to design and develop chalcogenide perovskite PV absorbers. First-principles calculation will be used to search for the material composition that leads to the optimal band gap and excellent optical absorption. Materials will be synthesized in both powder and thin-film forms. The structure, band gap, optical absorption and carrier transport will be systematically studied, and used as feedbacks for optimization of growth parameters and material properties. The expected outcome of this one year project is the development of PV absorbers with a band gap matched to the solar spectrum (~1.3 eV), high absorption coefficient (> 10^5 cm^{-1}), high carrier mobility and long diffusion length (> 1 μm).

Summary of Statement of Project Objectives (SOPO):

The main tasks and objectives of this one-year project are:

Task 1: Synthesis of chalcogenide perovskite powder and screening of substrates

• Milestone 1.1 (end of 3rd month): One suitable substrate for chalcogenide perovskite thin film deposition without detrimental defects as described above.

• Milestone 1.2 (end of 3rd month): Alloyed chalcogenide perovskite powder samples with tunable band gap from 1.1 to 1.8 eV.

Task 2: Fabrication of chalcogenide perovskite thin films

• Milestone 2.1 (end of 6th month): One chalcogenide perovskite thin film with an optical bandgap of 1.1-1.8 eV and a carrier concentration of 10^{15}-10^{18} cm^{-3}.

Task 3: Optimization of synthesis, optical and electronic properties of thin films

• Milestone 3.1 (end of 9th month): Growth parameters for thin films without detrimental deep level (> 0.2 eV from band edges) defects (predicted by theory, validated by experiment).

• Milestone 3.2 (end of 9th month): One chalcogenide perovskite thin film with a thickness of 0.5-2 μm, band gap of ~ 1.1-1.8 eV and absorption coefficient >1×10^4 cm^{-1}.

Task 4: Low temperature deposition and chemical stability of thin films

Final Milestone (end of project): One green and stable chalcogenide perovskite material in thin film form that possesses suitable band gap (1.1-1.8 eV) and high absorption coefficient (>1×10^4 cm^{-1}). One sample that has less than 10% change in band gap and absorption coefficient after 3 months exposure to ambient air and moisture. A theory-led manuscript on recombination-center defects and a paper on synthesis and characterization of chalcogenide perovskite thin films to a peer-reviewed journal.

Project Results and Discussion:

Stability and band gap tuning of $BaZrS_3$ at high pressure

We studied the effect of hydrostatic pressure on $BaZrS_3$, a prototypical chalcogenide perovskite with potential photovoltaic applications. Ab-initio density functional theory calculations were preformed to predict the allowed Raman phonons, their intensities, and their shift in frequency with pressure. Raman spectroscopy was used to investigate the effect of pressure, up to 8.9 GPa at room temperature and up to 6.8 GPa at 120K. In general, good agreement was found between experiment and theory. No phase changes were observed in the range studied. Our work confirms the structural stability of $BaZrS_3$. The stability against volume compression further suggests the possibility of cation alloying for band gap engineering for photovoltaic applications.

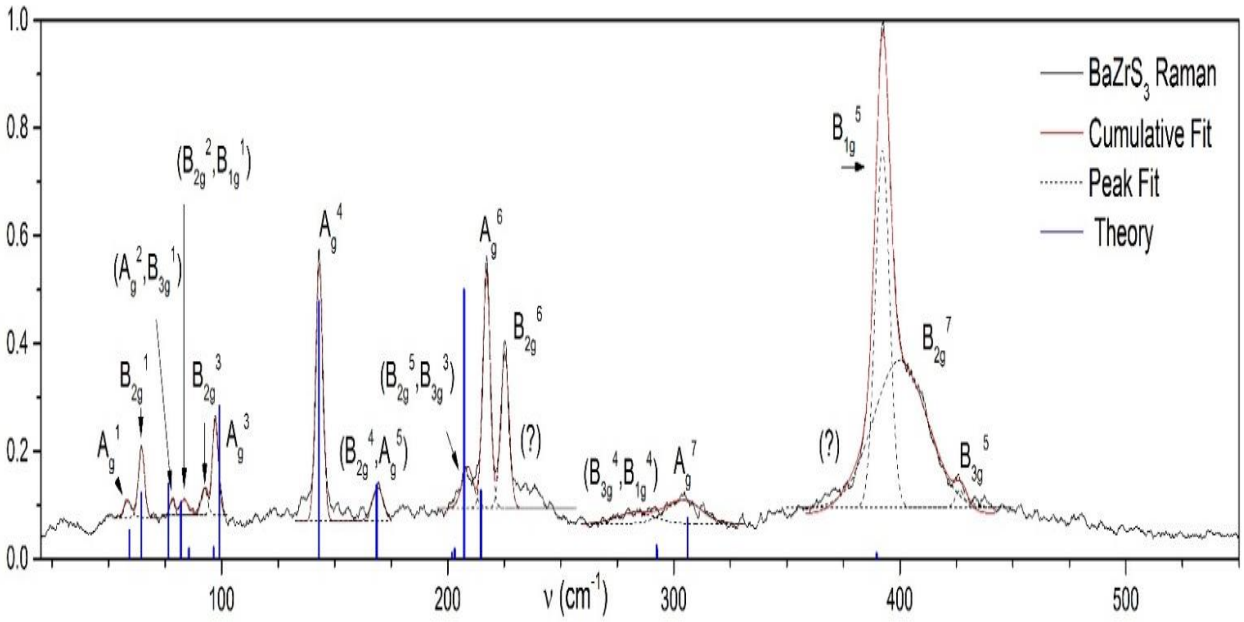

Fig. 1. Measured Raman spectrum (grey) of $BaZrS_3$ at 14 K and P = 0 GPa. Dashed and red curves are best fit results for the individual peaks and the cumulative spectrum, respectively. Labels give the peak phonon assignments based on comparison with the results of our DFT calculations. Question marks designate unassigned weak features that may arise from two-phonon scattering. Vertical lines indicate the theoretical strength of modes for which the DFT calculated relative intensity exceeds 2%.

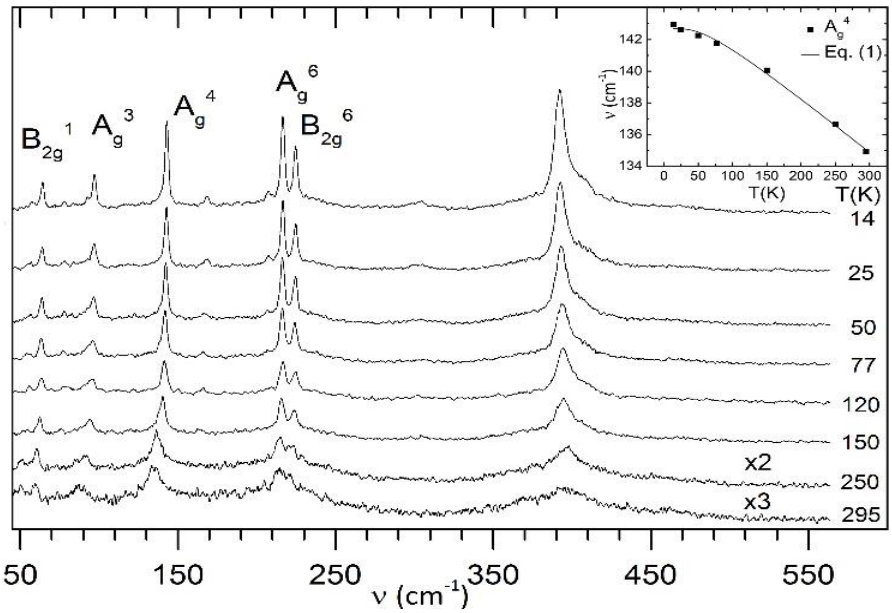

Fig 2. $BaZrS_3$ Raman data taken at temperatures from 14 K to 295 K. Gaussian line shape fits are used to determine peak positions. Inset shows sample fit of a standard temperature-shift relation for the A_g^4 peak.

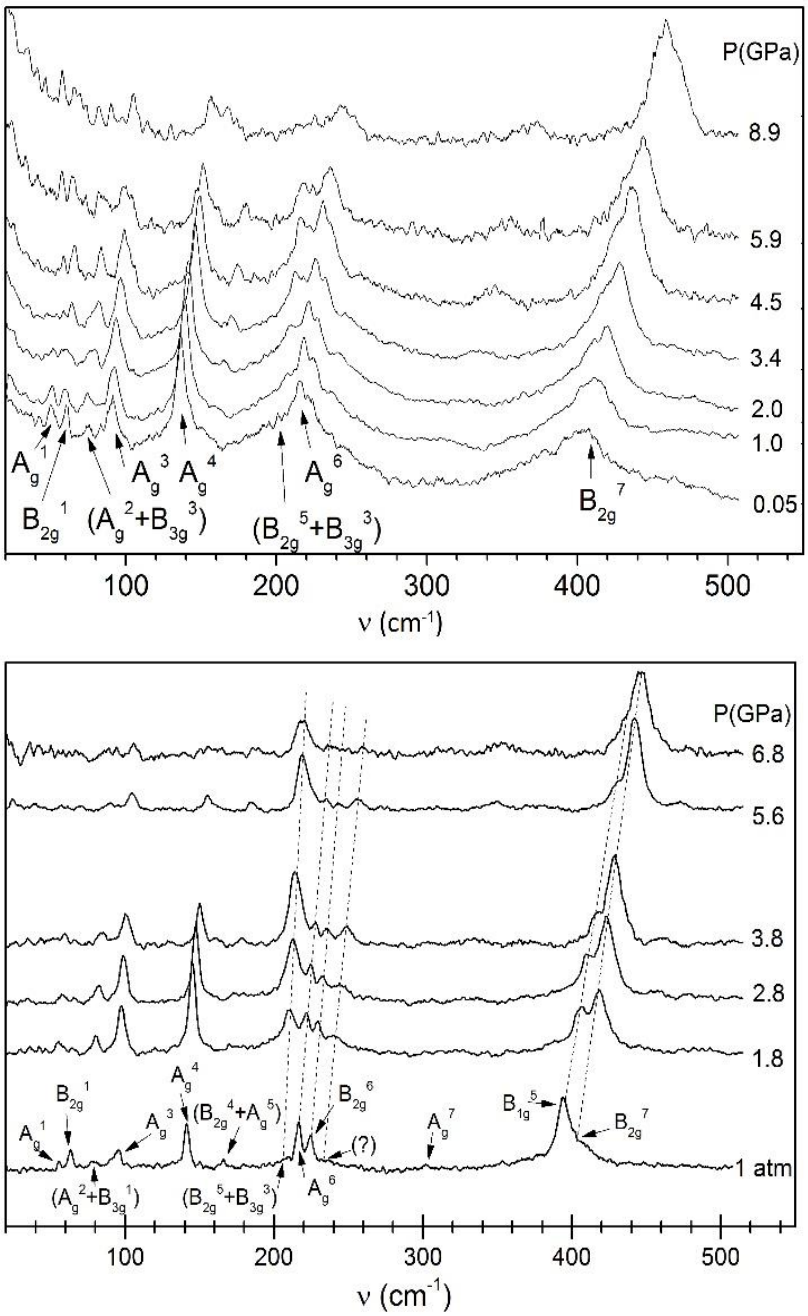

Fig 3. Pressure-Raman spectra of $BaZrS_3$ recorded at a) 295 K, and b) 120 K. Phonon assignments are given for the peaks that can be followed with pressure. Feature marked by (?) is unassigned. Dashed lines are guides to the eye showing shift of closely spaced peaks.

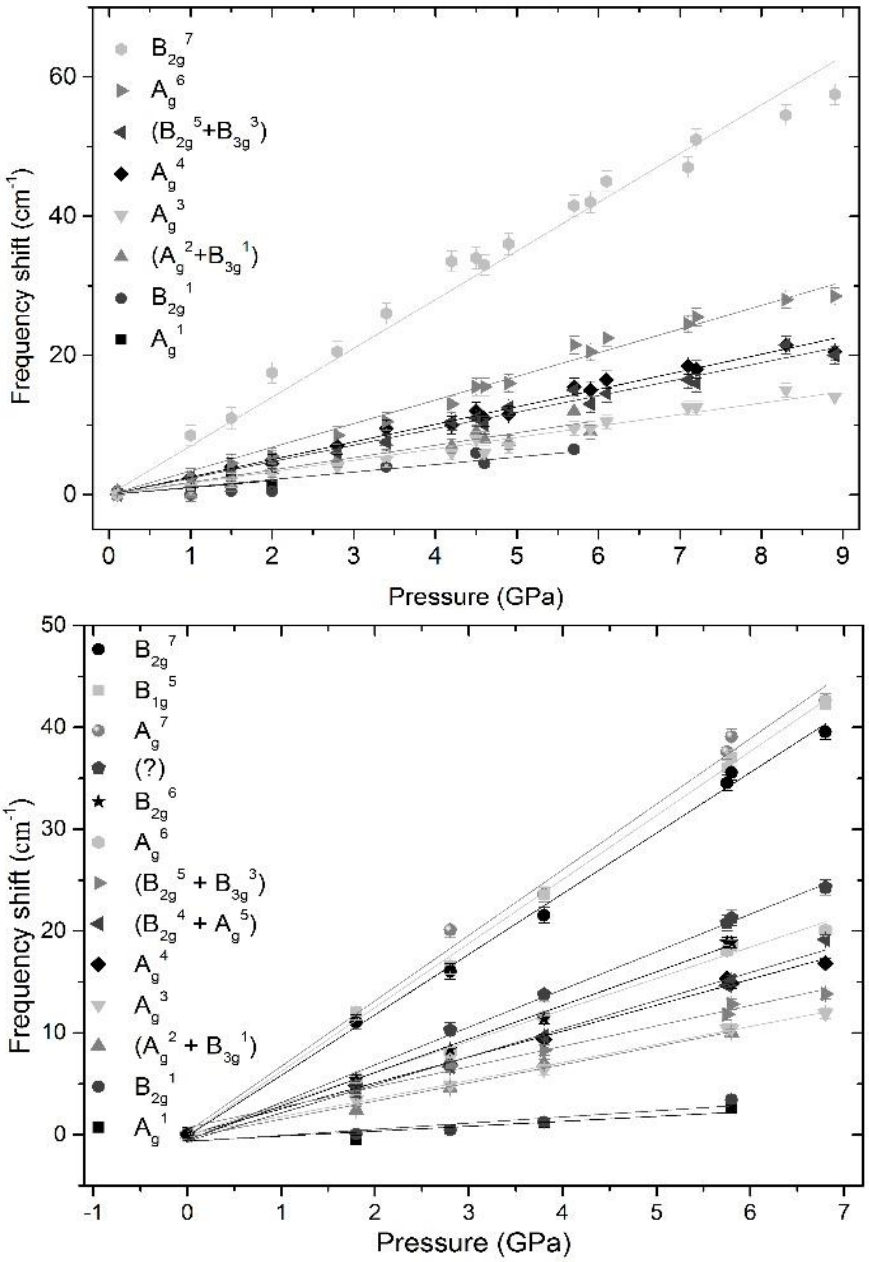

Fig 4. Frequency shifts with pressure of the observed Raman peaks in Figure 3 for a) 295K, and b) 120K. Peak positions are determined by Gaussian line shape fits. The mode correspondence of the plots follows the legends at left. The lines show the best linear fits to the data points.

Band gap tuning of $BaZrS_3$ by Ti-alloying

We investigated the effect of Ti-alloying of $BaZrS_3$ to tune its band gap. We observed systematic change of lattice parameters with increasing Ti concentration. The UV-vis measurements showed systematic red-shift of the absorption spectra. The lowest band gap obtained is 1.4 eV, matching the optimal band gap for a single junction cell. Doping of Ti over 10% yields phase separation, which is consistent with theoretical studies.

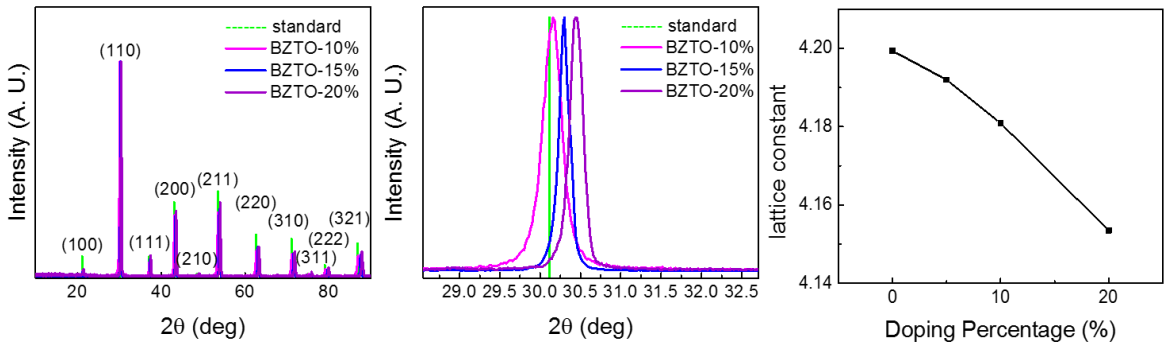

Fig. 5. Ti-doped $BaZrO_3$ was used for the preparation of $BaZrS_3$ by sulfurization. As can be seen, with increasing Ti-alloying concentration, the lattice constant decreases monotonically, suggesting Ti substitution of Zr.

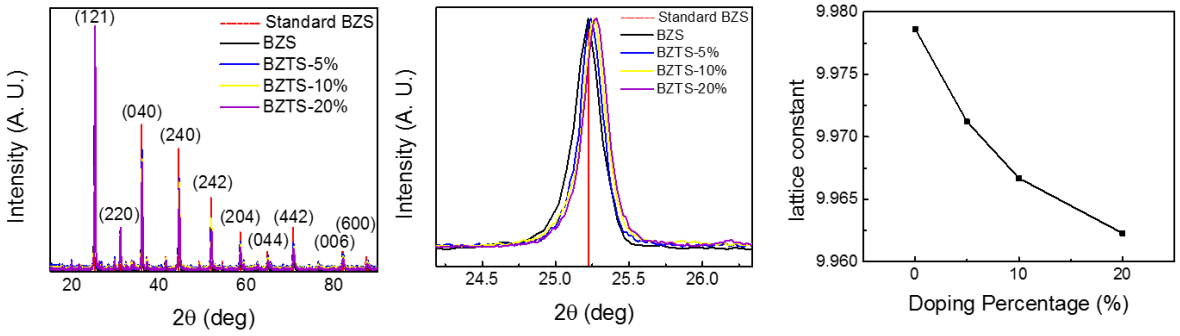

Fig. 6. After sulfurization, the lattice constant of Ti-doped $BaZrS_3$ showed similar trend to that of Ti-doped $BaZrO_3$. At Ti-alloying concentration > 10%, secondary phases are detected by XRD.

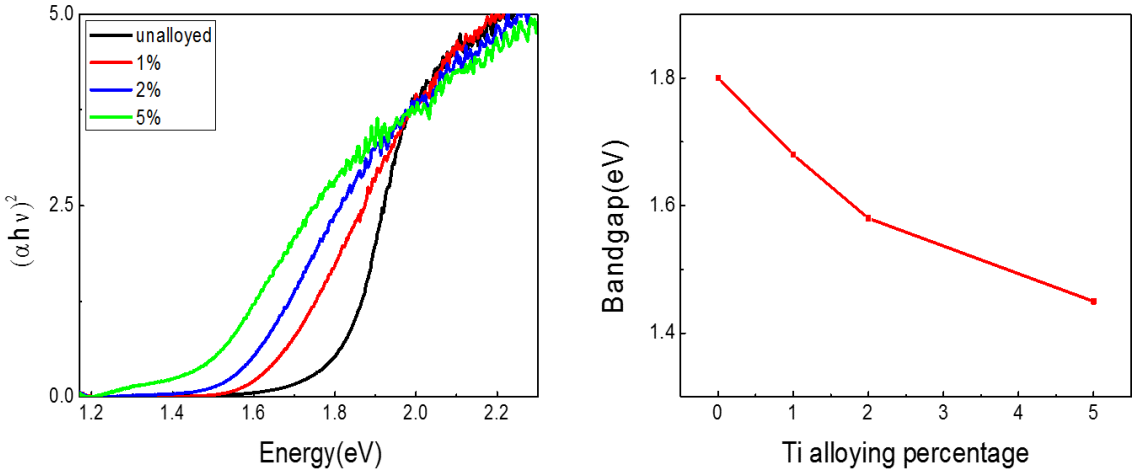

Fig. 7. With increasing Ti-alloying concentration, the band gap systematically decreases. At 5% Ti, the band gap is ~ 1.45 eV, close to the optimal value for a single junction solar cell.

Fabrication of $BaZrS_3$ thin film by PLD and sulfurization

We synthesized $BaZrS_3$ thin films by sulfurization of pre-deposited BaZrO3 thin films. The thin films possess the expected structure as identified by XRD patterns and Raman spectra. The optical absorption showed the expected band gap. The films show strong photoluminescence, confirming the direct band gap nature of the material, and further suggest that the material is of reasonable carrier and defect density.

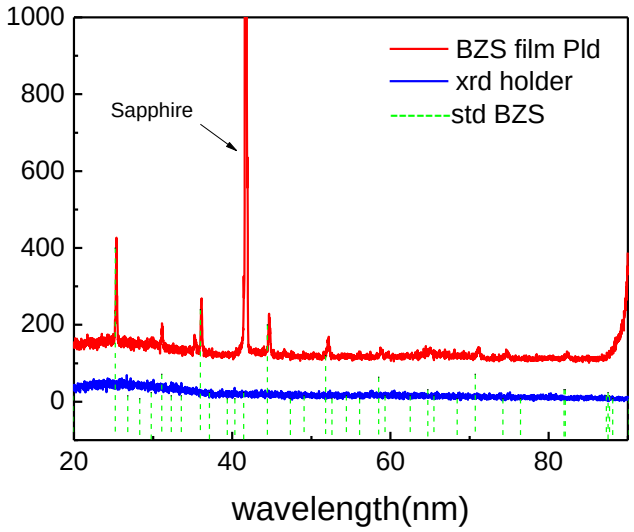

Fig. 8. XRD shows that the films deposited by PLD of oxide followed by sulfurization retains the distorted perovskite structure expected for $BaZrS_3$.

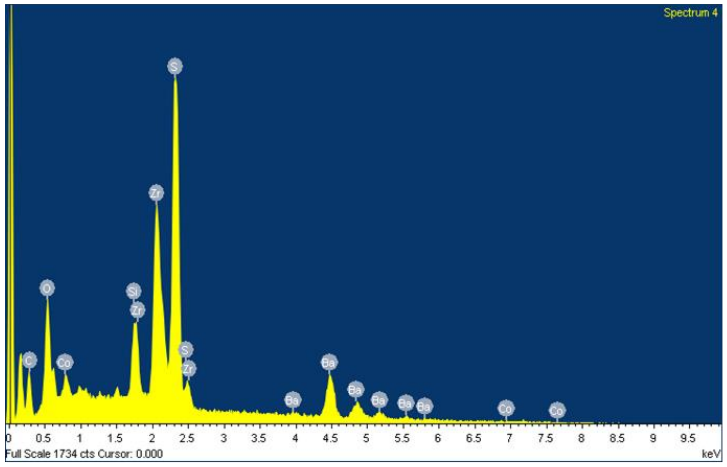

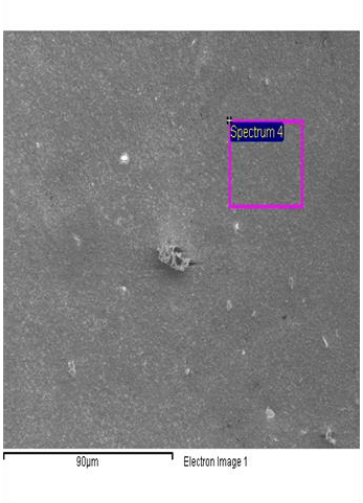

Element	Weight%	Atomic%	
C K	6.36	23.23	
O K	6.22	17.04	
Si K	2.97	4.64	
S K	22.68	31.02	
Co K	0.00	0.00	
Zr L	26.99	12.97	
Ba L	34.78	11.11	
Totals	100.00		

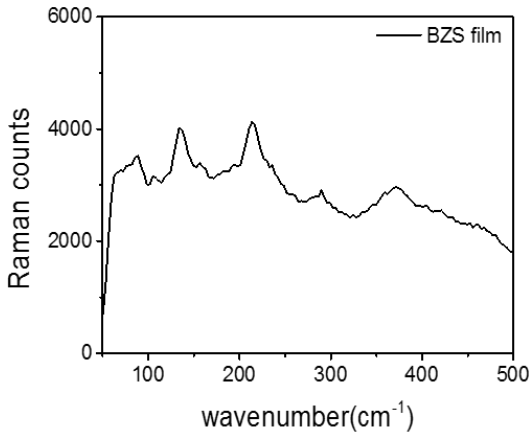

Fig. 9. Composition measured by EDX is close to stoichiometry. Raman spectra also showed expected features.

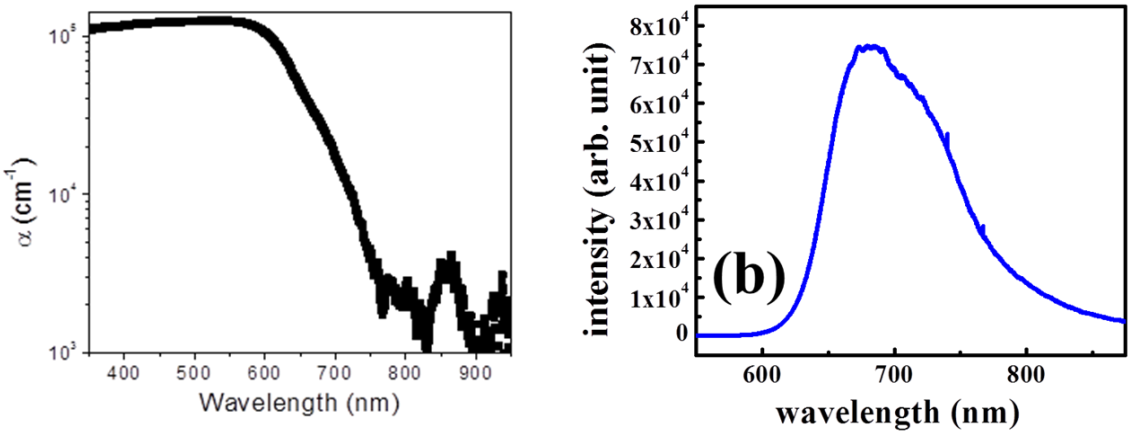

Fig. 10. UV-vis spectra showed expected band gap. The absorption coefficient is calculated to be > $10^5 cm^{-1}$. The films show strong photoluminescence, consistent with its direct band gap nature.

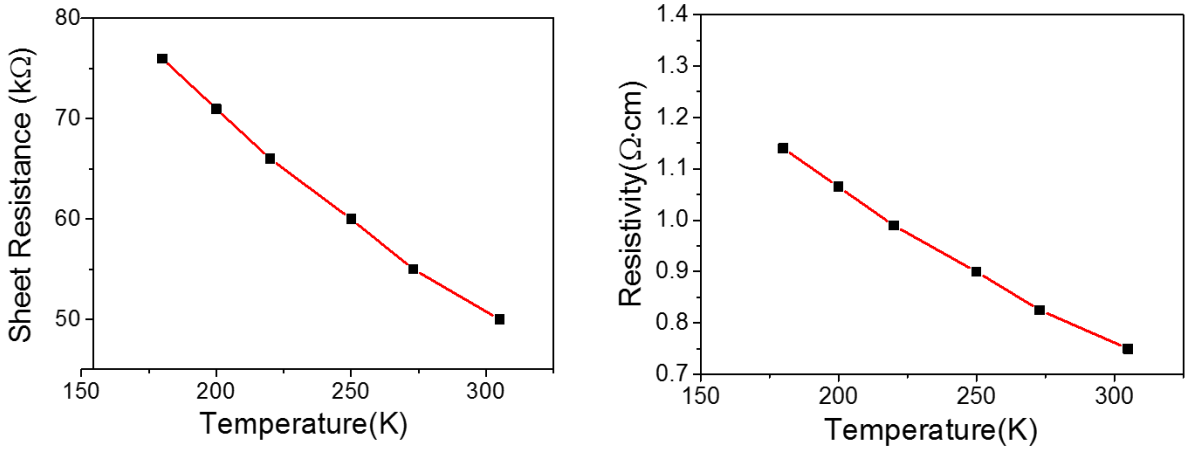

Fig. 11. Temperature dependence of sheet resistance and resistivity has been fitted by a thermal activation model. The activation energy is extracted to be 14.7 meV, suggesting shallow defect levels.

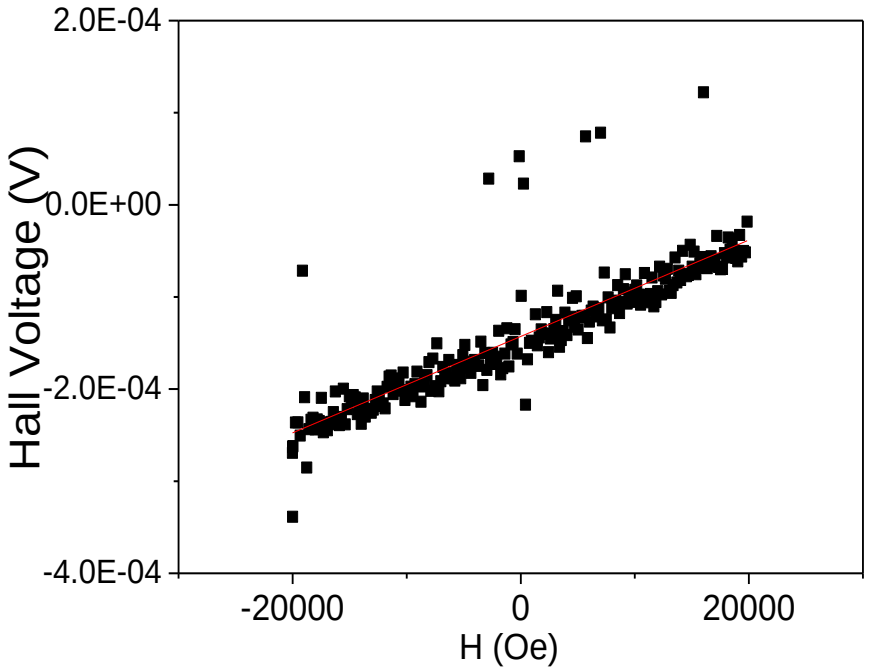

Fig. 12. Initial Hall effect measurements reveals that the carrier is p-type. This needs to be confirmed since we expect n-type conductivity due to S vacancy. Combining Hall and resistivity measurements, we extracted carrier concentration of ~ 8×10^{17}cm^{-3} and mobility of ~ 9.39 cm^2/Vs.

Fabrication of $BaZrS_3$ thin film by direct PLD deposition of $BaZrS_3$

Sulfurization of oxide film requires temperatures higher than 1000 C, which is not compatible with device fabrication. In an attempt to decrease the deposition temperature, we developed a method to deposit BaZrS3 films directly. The procedure is as follows: 1. Synthesis of $BaZrS_3$ powder by sulfurization of $BaZrO_3$ powder; 2. Press of $BaZrS_3$ powder to make PLD target; 3. Deposition of thin films using BZS target.

Fig. 13. （left to right） The $BaZrO_3$ powder; the as-synthesized $BaZrS_3$ powder; the $BaZrS_3$ target and the deposited $BaZrS_3$ film on sapphire substrate, respectively.

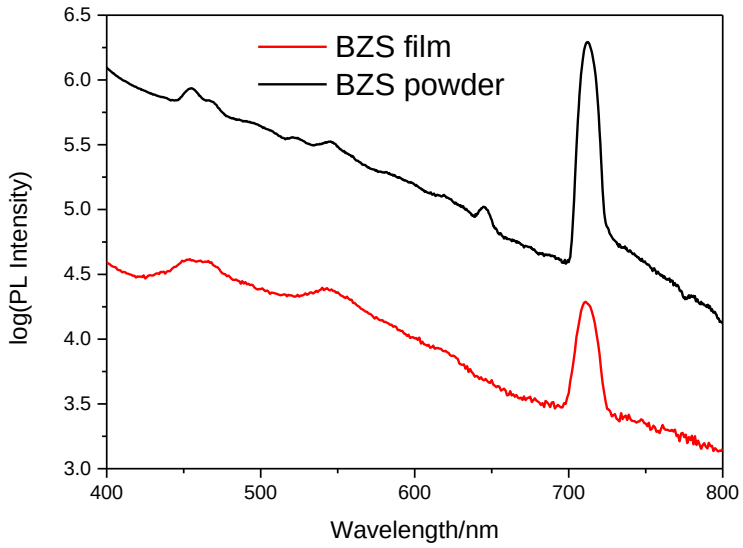

Fig. 14. The photoluminescence spectra of BZS film compared to that of the powder sample.

Computational study of defect properties of $BaZrS_3$

We calculated the formation energies of possible point defects in $BaZrS_3$ using density functional theory. The formation energies were calculated as a function of chemical potentials of the constituent elements. The allowed chemical potential region for the three elements was carefully determined. Within this allowed region, we were able to identify the low-energy point defects. We also calculated the formation energies as a function of Fermi energy. Based on these calculations, we can determine possible deep levels that could serve as recombination centers and lower the efficiency of PV devices.

Actually, our calculations showed that $BaZrS_3$ may not have deep-level intrinsic defects, this is different from a recent publication [11], where it was found that some defects, such as S-on-Zr (S_{Zr}), may have a deep (0/-) transition level. We carefully examined their results and found that the deep level is a result of using too large Hubbard U value (4.5 eV) for Zr 4d electrons. Instead of empirically selecting the U value, we calculated the U value from first-principles and found a value of 1.65 eV only. With this newly calculated U, we did not observe deep levels in our calculations.

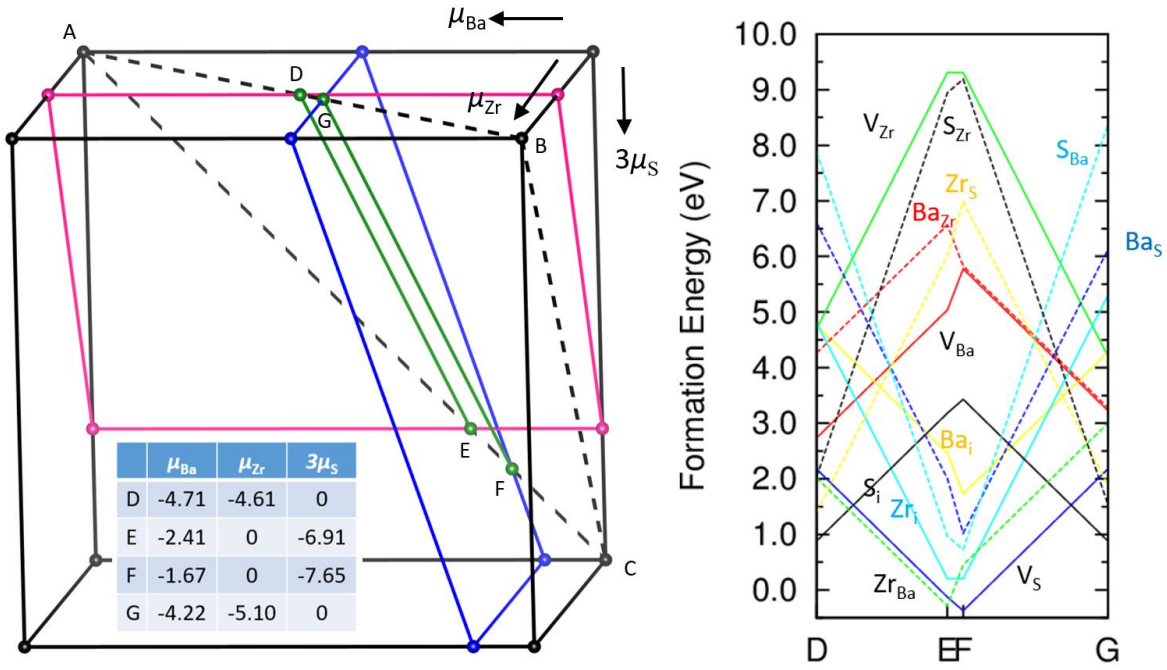

	μ_{Ba}	μ_{Zr}	$3\mu_S$
D	-4.71	-4.61	0
E	-2.41	0	-6.91
F	-1.67	0	-7.65
G	-4.22	-5.10	0

Fig. 16. (Left) The green region marked by points D, E, F, and G shows the allowed region of chemical potentials of Ba, Zr and S ensuring that $BaZrS_3$ is thermodynamically stable. The inset shows the coordinates of the points D, E, F, and G. The unit is in eV. (Right) Calculated defect formation energy for all possible point defects in $BaZrS_3$, as a function of chemical potential. Defects having the lowest formation energies are S vacancy (V_S) and Zr on Ba anti-sites (Zr_{Ba}). Other defects, such as Zr interstitial (Zr_i), S interstitial (S_i), S on Ba (S_{Ba}), and Ba on S (Ba_S) could also have formation energy that is lower than or close to 1 eV.

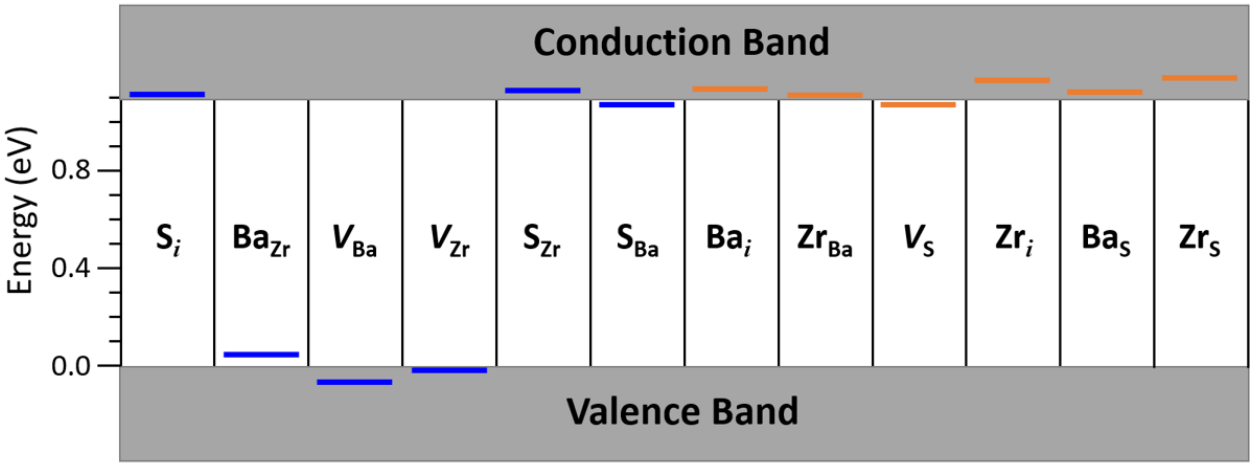

Fig. 17. Using a Hubbard U value of 1.65 eV, as calculated from first-principles, we performed PBE+U calculations to determine the defect transition levels in $BaZrS_3$. It was found that for all the point defects, the (0/+) and (0/-) transition levels, which are the potential recombination centers, are shallow defects. This result is different from a recent study using a significant larger U value (4.5 eV), where it was predicted that some defects are deep-level defects, such as S_{Zr} anti-site.

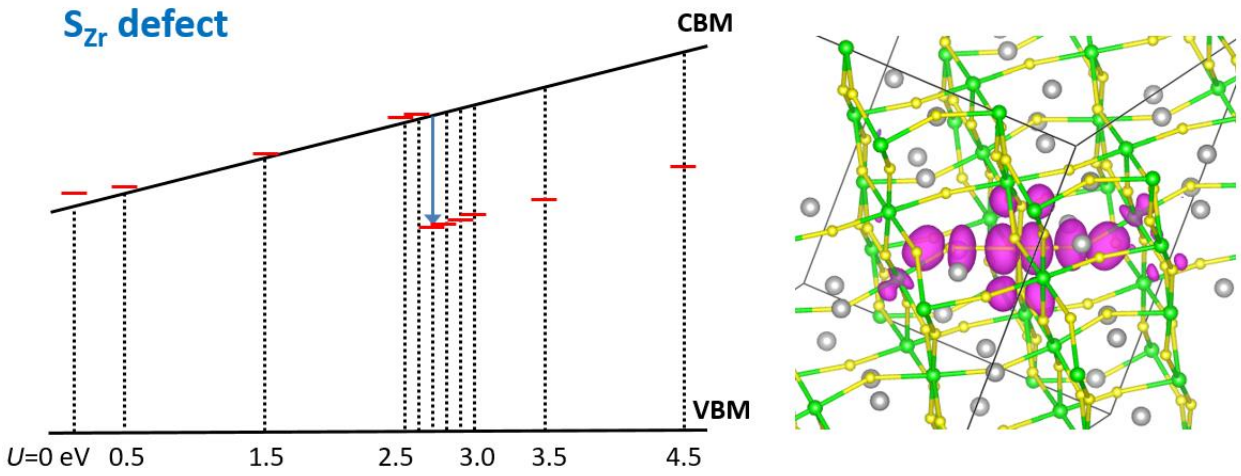

Fig. 18. We studied the calculated transition level of S_{Zr} defect as a function of U value. It was found that the defect suddenly changed from a shallow to a deep level as the U value is above 2.7 eV. The shallow-to-deep transition is accompanied by a localization of the gap state (right panel). However, as stated above, the U value according to our first-principles calculation is only about 1.65 eV, which means that the deep level may not be real. We tend to conclude that in $BaZrS_3$, the intrinsic defects are all shallow defects, which do not serve as recombination centers.

Conclusions: We confirmed structural stability of the chalcogenide perovskite $BaZrS_3$ through high-pressure Raman studies. Manuscript has been published in Phys. Rev. Appl. 8, 044014 (2017). Reduced band gap to 1.45 eV has been achieved by Ti-alloying of $BaZrS_3$, which is close to optimal value for a single junction solar cell (Manuscript in preparation). Synthesized $BaZrS_3$ thin films show desired structure and band gap. Its direct band gap is confirmed by PL. Its optical absorption coefficient is > 10^5 cm^{-1}, carrier concentration is ~$8\times10^{17}cm^{-3}$ and mobility is ~9.4 cm^2/Vs. These initial results on films are encouraging. A concern is the rough film surface morphology, due to the high temperature sulfurization process. This may lead to error in transport measurements. Furthermore, the high-temperature process is not compatible with device fabrication. To address this problem, we plan to deposit $CaZrSe_3$ thin film (band gap of 1.3 eV corresponding to the optimal band gap for a single-junction solar cell) using a modified MBE system incorporating a high-temperature cell for Zr evaporation.

Budget and Schedule:

III. Spending Summary by Budget Category					
	Approved Budget per SF-424A			Actual Expenses	
Budget Categories per SF-424a	BP 1	BP 2	BP 3	This Quarter	Cumulative
a. Personnel	43485			$165	$44,962
b. Fringe Benefits	13123			$90	$11,902
c. Travel	3000			$75	$3,459
d. Equipment	11000			$0	$26,641
e. Supplies	10000			$0	$8,641
f. Contractual	126255			$440	$126,909
g. Construction					
h. Other	20744			$349	$5,055
i. Total Direct Charges	$227,607	$0	$0	$1,119	$227,665
j. Indirect Charges	57864			$404	$57,815
k. Total Charges	$285,471	$0	$0	$1,523	$285,480
DOE Share	224814			$1,116	$224,814
Cost Share	60657			$407	$60,666
Cost Share Percentage	21.2%	#DIV/0!	#DIV/0!	26.7%	21.3%

Federal share: $224,814, cost share: $60,666.17, amounts spent: 285,480.17.

The main deviation from the spending plan is the re-budget of $20,000 for the purchase of an e-gun for MBE deposition of $CaZrSe_3$ thin films.

1.1	One suitable substrate for chalcogenide perovskite thin film deposition without detrimental defects as described above	Yiyang Sun	7/1/16	7/31/16
1.2	Alloyed chalcogenide perovskite powder samples with tunable band gap from 1.1 to 1.8 eV	Hao Zeng	7/1/16	7/31/16
2.1	One chalcogenide perovskite thin film with an optical bandgap of 1.1-1.8 eV and a carrier concentration of 10^{15}-10^{18} cm^{-3}		10/1/2016	10/31/16
3.1	Growth parameters for thin films without detrimental deep level (> 0.2 eV from band edges) defects (predicted by theory, validated by experiment)	Hao Zeng/Yiyang Sun	10/1/16	1/31/17
3.2	One chalcogenide perovskite thin film with a thickness of 0.5-2 mm, band gap of ~ 1.1-1.8 eV and absorption coefficient >1´10^4 cm^{-3}	Hao Zeng	1/1/2017	1/31/17
final	One green and stable chalcogenide perovskite material in thin film form that possesses suitable band gap (1.1-1.8 eV) and high absorption coefficient (>1´10^4 cm^{-3}). One sample that has less than 10% change in band gap and absorption coefficient after 3 months exposure to ambient air and moisture. A theory-led manuscript on recombination-center defects and a paper on synthesis and characterization of chalcogenide perovskite thin films to a peer-reviewed journal	Hao Zeng/Yiyang Sun	7/1/16	4/30/17

The main deviation from the original schedule was a few months delay due to availability of funding due to contracting process.

Path Forward:

Deposition of $CaZrSe_3$ thin film using MBE: The highest quality chalcogenide perovskite thin films that can be made, with correct stoichiometry and single crystalline-like, is probably by molecular beam epitaxy, if a suitable substrate can be identified for epitaxial growth. The difficulty is that most MBE systems are not equipped with an ultra-high temperature cell that can be used to evaporate Zr metal. We have modified our MBE system by installing an e-beam evaporation cell. Systematic optimization of deposition parameters is to be performed.

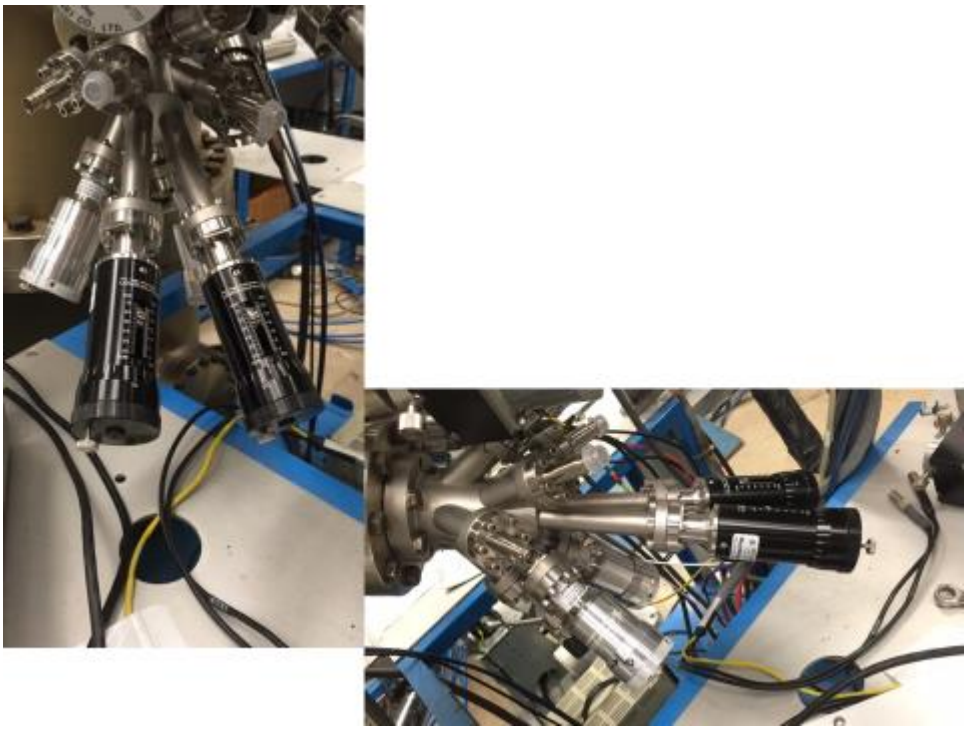

Fig. 15. The e-beam evaporation cell installed on the MBE system.

Acknowledgment: “This material is based upon work supported by the Department of Energy under award number DE-EE0005398”

References:

[1] A. Kojima, K. Teshima, Y. Shirai, T. Miyasaka, “Organometal halide perovskites as visible-light sensitizers for photovoltaic cells”, *J. Am. Chem. Soc.* **131**, 6050 (2009).
[2] Research Cell Record Efficiency Chart, https://www.nrel.gov/pv/
[3] M. Grätzel, “The light and shade of perovskite solar cells”, *Nature Mater.* **13**, 838 (2014).
[4] W. Tress, N. Marinova, T. Moehl, S. M. Zakeeruddin, M. K. Nazeeruddin and M. Grätzel, “Understanding the rate-dependent J–V hysteresis, slow time component, and aging in CH3NH3PbI3 perovskite solar cells: the role of a compensated electric field", *Energy Environ. Sci.* **8**, 995 (2015).
[5] A. Pisoni, J. Jaćimović, O. S. Barišić, M. Spina, R. Gaál, L. Forró, and E. Horváth, “Ultra-Low Thermal Conductivity in Organic–Inorganic Hybrid Perovskite CH3NH3PbI3”, *J. Phys. Chem. Lett.* **5**, 2488 (2014).
[6] H. Hahn and U. Mutschke, “Untersuchungen über ternäre Chalkogenide. XI. Versuche zur Darstellung von Thioperowskiten,” *Zeitschrift für Anorg. und Allg. Chemie* **288**, 269 (1957).
[7] T. Nitta, K. Nagase, and S. Hayakawa, “Formation, Microstructure, and Properties of Barium Zirconium Sulfide Ceramics,” *J. Am. Ceram. Soc.* **53**, 601 (1970).
[8] A. Clearfield, “The synthesis and crystal structures of some alkaline earth titanium and zirconium sulfides,” *Acta Crystallogr.* **16**, 135 (1963).
[9] Y. Wang, N. Sato and T. Fujino, “Synthesis of BaZrS3 by short time reaction at lower temperatures”, *J. Alloys Comp.* **327**, 104 (2001).

[10] Y. Y. Sun, M. L. Agiorgousis, P. Zhang, and S. B. Zhang, “Chalcogenides perovskites for photovoltaics”, *Nano Lett.* **15**, 581 (2015).
[11] W. Meng, B. Saparov, F. Hong, J. Wang, D. B. Mitzi, and Y. Yan, “Alloying and Defect Control within Chalcogenide Perovskites for Optimized Photovoltaic Application”, *Chem. Mater.* **28**, 821 (2016).
[12] S. Pereraa, H. Hui, C. Zhao, H. Xue, F. Sun, C. Deng, N. Gross, C. Milleville, X. Xu, D. F. Watson, B. Weinstein, Y.-Y. Sun*, S. Zhang, and H. Zeng, “Chalcogenide perovskites – an emerging class of ionic semiconductors”, *Nano Energy* **22**, 129 (2016).
[13] S. Niu, H. Huyan, Y. Liu, M. Yeung, K. Ye, L. Blankemeier, T. Orvis, D. Sarkar, D. J. Singh, R. Kapadia, J. Ravichandran, “Bandgap Control via Structural and Chemical Tuning of Transition Metal Perovskite Chalcogenides”, *Adv. Mater.* **29**, 1604733 (2017).